ISSN: 1992-8645 www.jatit.org E-ISSN: 1817-3195

# HIGHLY NONLINEAR RIGID FLEXIBLE MANIPULATOR STATE ESTIMATION USING THE EXTENDED AND THE UNSCENTED KALMAN FILTERS

[1] MOHAMMED BAKHTI, [2] BADR BOUOULID IDRISSI

[1,2] Moulay Ismail University, Ecole Nationale Supérieure d'Arts et Métiers,

BP 4024, Marjane II, Beni Hamed, 50000, Meknes, Morocco.

E-mail: [1] mdbakhti@yahoo.fr, [2] badr.bououlid@gmail.com

**ABSTRACT**

This paper focuses on the highly nonlinear rigid-flexible manipulator state estimation using the Extended Kalman Filter and the Unscented Kalman Filter. The Hamilton's principle is used to derive the manipulator equations, the Euler-Bernoulli assumption is considered to model the flexible link, and the elastic movement is approximated using the assumed modes method. The simulation study compares the efficiency of the state estimation quantified by the estimation mean squared error and the time required by the filters to converge.

**Keywords:** *Extended Kalman Filter, Rigid-Flexible Manipulator, Nonlinear Filtering, State Estimation, Unscented Kalman Filter.*

## 1. INTRODUCTION

Rigid-flexible manipulators are a promising alternative to rigid-rigid ones due to their greater payload to manipulator weight ratio, higher operation speed, larger work space, lower energy consumption and safer operability. However, they exhibit disadvantages of deflection associated with structural flexibility and vibration problem [1]. Their modeling approaches and their control/observation strategies must consider both the rigid body and the flexible degrees of freedom [2].

The Hamilton's principle is one of the most used approaches when modeling the flexible manipulators. The deformation model of the flexible links is usually based on the Euler – Bernoulli beam theory, and the elastic degrees of freedom are approximated using either the assumed mode method or the finite element method. In general, only first few vibration modes play a significant role in the dynamic equations formulation. As actuators, usually DC motors are used at the manipulator joints due to their simple control scheme.

Most of the active vibration control strategies require the state feedback, and many nonlinear observer formulations have been addressed for the flexible manipulators. To estimate the elastic degrees of freedom and their time derivatives, a nonlinear high gain observer has been developed by [3], and the sliding mode theory has been investigated by [4] to design both a controller and an observer for the tip positioning problem. Distributed observers have been presented by [5, 6] to estimate infinite dimensional states requiring only the boundary values measured by sensors. An extended state observer was proposed for the trajectory tracking control of a flexible-joint robotic system by [7], and the Extended Kalman Filter has been used by [8] to give an estimate of the environmental forces.

Using the Taylor series expansion, the optimal way a linear Kalman filter provide the mean and covariance of a linear system state can be extended to nonlinear ones. The Extended Kalman Filter (EKF) is based on linearizing the nonlinear system around the state nominal trajectory [9]. The optimal solution to the nonlinear filtering requires the filter to give an accurate estimate for all the probability distribution function (pdf) moments, and, thus, the problem is infinite dimensional [10]. However, when the noises corrupting the system are assumed to be Gaussian, the mean and covariance are sufficiently describing the state pdf [11]. Unfortunately, the EKF requires the nonlinear prediction and measurement function jacobians to be evaluated repeatedly at each time step [12], and this may cause the results to be unreliable and the implementation to be difficult.

A diversion from evaluating the jacobians is allowed by the Unscented Kalman Filter (UKF) [13]. As an alternative, a small set of points, called the sigma-points, are carefully chosen to capture the mean and covariance of the state before they undergo the system nonlinearities. Once transformed, those points are used to evaluate the mean and covariance of the state to be estimated. Contrarily to the Monte Carlo method, the samples are not drawn at random, yet they are deterministically selected so that they capture the essential information about the state pdf.

Preceding research paper addressed the nonlinear optimal state estimation under parametrice uncertianties based on the EKF and the UKF for a one-link flexible manipulator [14,15]. Based on simplifying assumptions, a linear model of the flexible manipulator was targetted by a Model Predictive Control scheme associated to a state estimation based on Kalman filter in [16].

The main contribution of this paper is to compare the EKF and the UKF algorithms when used to estimate the state of a highly nonlinear 2 Degrees of Freedom (2DOF) rigid-flexible manipulator. The analyzed motion of the manipulator is fully described by the rigid body motion, and the vibration motion. Thus the state vector consists of the shoulder joint angle, the elbow joint angle, the first modal coordinate and their respective time derivatives. The flexible link deformation is described using the Euler-Bernoulli theory, the elastic degree of freedom is approximated using the assumed mode method, and the system equations are derived using Hamilton's principle.

In the next section, the mathematical model for the rigid-flexible manipulator is derived, while in section 3, the EKF and the UKF principles and algorithms are detailed. Simulation results are displayed and discussed in section 4, and conclusion are outlined in section 5.

## 2. MATHEMATICAL MODELING OF THE RIGID-FLEXIBLE MANIPULATOR

The shoulder and elbow joint angular positions, driven by servo motors, are respectively $\theta_1$ and $\theta_2$, and $L_1$ denotes the length of the rigid link. The radius of the rigid hub is $r$ and the elastic displacement is $w(x,t)$, where $x$ is the non deformed point location on the flexible link.

Two reference systems are defined:

1. An inertial system: $(X,Y,Z)$ with its $Z$-axis aligned with the shoulder servomotor shaft, and the $X$-axis aligned with the home position of the rigid manipulator.
2. A rotating system: $(x,y,Z)$, as local coordinate system, attached to the rigid hub and its $x$-axis tangent to the flexible link at the shaft of the elbow servomotor.

The two-link rigid-flexible manipulator geometry and coordinates are shown in Figure 1.

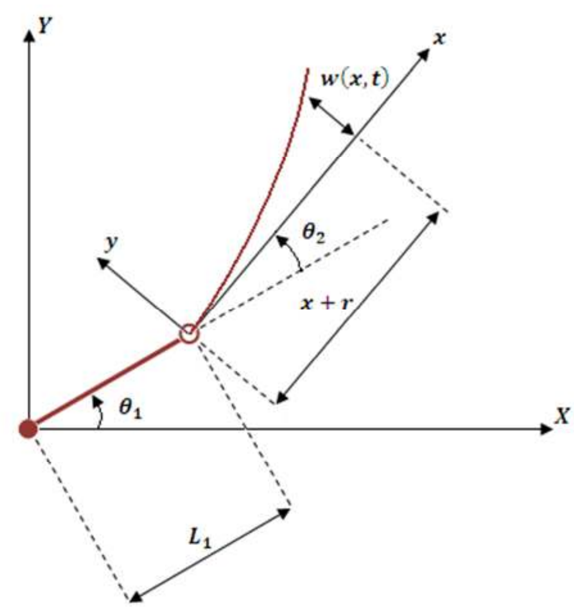


*Figure 1: The Two-link Rigid-Flexible Manipulator Geometry and Coordinates*

The gravity is not considered since the manipulator moves in the horizontal plane, and the flexible link is assumed to be an Euler–Bernoulli beam where the longitudinal deformation is neglected.

Kinematics of the system, relative to the inertial system, may be described by the following position vector:

$$\vartheta = \begin{bmatrix} \vartheta_x \\ \vartheta_y \end{bmatrix} =$$

ISSN: 1992-8645 www.jatit.org E-ISSN: 1817-3195

$$\begin{bmatrix} L_1 \cos(\theta_1) + (x+r)\cos(\theta_1+\theta_2) - w\sin(\theta_1+\theta_2) \\ L_1 \sin(\theta_1) + (x+r)\sin(\theta_1+\theta_2) + w\cos(\theta_1+\theta_2) \end{bmatrix} \quad (1)$$

Thus:

$$\dot{\vartheta}^2 = \begin{bmatrix} \frac{d\vartheta_x}{dt} & \frac{d\vartheta_y}{dt} \end{bmatrix} \begin{bmatrix} \frac{d\vartheta_x}{dt} \\ \frac{d\vartheta_y}{dt} \end{bmatrix} = {L_1}^2{\dot{\theta}_1}^2 + \left((r+x)(\dot{\theta}_1+\dot{\theta}_2)+\dot{w}\right)^2 + 2L_1\dot{\theta}_1\left(\left((r+x)(\dot{\theta}_1+\dot{\theta}_2)+\dot{w}\right)\right)\cos(\theta_2) + \left(w(\dot{\theta}_1+\dot{\theta}_2)\right)^2 - 2L_1\dot{\theta}_1(\dot{\theta}_1+\dot{\theta}_2)w\sin(\theta_2) \quad (2)$$

Including the rigid link and the shoulder servomotor and hub inertia $I_1$ and $I_h$, with respect to the shoulder joint axis, the total kinetic energy of the system can be written as:

$$T = \frac{1}{2}I_1{\dot{\theta}_1}^2 + \frac{1}{2}I_h\left({\dot{\theta}_1}^2+{\dot{\theta}_2}^2\right) + \frac{1}{2}m_h{L_1}^2{\dot{\theta}_1}^2 + \frac{1}{2}\int_0^{L_2}\rho A\dot{\vartheta}^2dx \quad (3)$$

Where $\rho, A$ and $m_h$ are, respectively, the mass density of the flexible link, its cross section area and the elbow hub mass.

According to the Euler-Bernoulli assumption, the potential energy of the system is given by [17]:

$$P = \frac{1}{2}\int_0^{L_2} EI_2\left(\frac{\partial^2 w}{\partial x^2}\right)^2 dx + \frac{1}{2}\int_0^{L_2} F(x,t)\left(\frac{\partial \vartheta}{\partial x}\right)^2 dx \quad (4)$$

Where $E$ and $I$ are the flexible link Young's modulus and its moment of inertia. $F(x,t)$ is given for a uniform beam by [18]:

$$F_c(x,t) = \frac{1}{2}\rho{\dot{\theta}_2}^2({L_2}^2-x^2) + \rho{\dot{\theta}_2}^2 r(L_2-x) \quad (5)$$

Once the kinetic and potential energies of the system are explicited, the system equations are derived using Hamilton's principle [19]:

$$\int_{t_0}^{t_f}(\delta T - \delta P + \delta W)dt = 0 \quad (6)$$

Where $\delta W$ is the virtual work done by the joint torques $\tau_1$ and $\tau_2$, at the shoulder and the elbow joints respectively.

The Hamilton's principle results on the following equations in which a dot denotes the derivative with respect to time, and a prime denotes the derivative with respect to the spatial variable $x$:

$$\begin{aligned}(I_1 + m_h{L_1}^2)\ddot{\theta}_1 + I_h(\ddot{\theta}_1+\ddot{\theta}_2) + \frac{1}{2}\int_0^{L_2}\rho A\Big((r+x)^2(\ddot{\theta}_1+\ddot{\theta}_2) + \ddot{w}(r+x) + L_1\ddot{\theta}_1 \\ + 2w\dot{w}(\dot{\theta}_1+\dot{\theta}_2) + w^2(\ddot{\theta}_1+\ddot{\theta}_2) \\ + 2L_1(r+x)\ddot{\theta}_1\cos(\theta_2) \\ - 2L_1(r+x)\dot{\theta}_1\dot{\theta}_2\sin(\theta_2) \\ - 2L_1\ddot{\theta}_1 w\sin(\theta_2) \\ - L_1(r+x)\dot{\theta}_2^2\sin(\theta_2) \\ - 2L_1\dot{w}(\dot{\theta}_1+\dot{\theta}_2)\sin(\theta_2) \\ - 2L_1 w\dot{\theta}_1\dot{\theta}_2\cos(\theta_2) \\ - L_1\dot{\theta}_2 w\cos(\theta_2) - \frac{1}{2}(L_2^2 - x^2 \\ + 2rL_2 - 2rx)w'^2(\ddot{\theta}_1+\ddot{\theta}_2) \\ - (L_2^2 - x^2 + 2rL_2 - 2rx)w'\dot{w}'(\dot{\theta}_1 \\ + \dot{\theta}_2)\Big)dx \\ = \tau_1 \quad (7)\end{aligned}$$

$$\begin{aligned}I_h(\ddot{\theta}_1+\ddot{\theta}_2) + \int_0^{L_2}\rho A\Big((r+x)^2(\ddot{\theta}_1+\ddot{\theta}_2) + \ddot{w}(r+x) \\ + 2w\dot{w}(\dot{\theta}_1+\dot{\theta}_2) + w^2(\ddot{\theta}_1+\ddot{\theta}_2) \\ + L_1(r+x)\ddot{\theta}_1\cos(\theta_2) \\ - L_1\ddot{\theta}_1 w\sin(\theta_2) \\ + L_1\dot{\theta}_1^2(r+x)\sin(\theta_2) \\ + L_1\dot{\theta}_1^2 w\cos(\theta_2) \\ - \frac{1}{2}(L_2^2 - x^2 + 2rL_2 - 2rx)w'^2(\ddot{\theta}_1 \\ + \ddot{\theta}_2) \\ - (L_2^2 - x^2 + 2rL_2 - 2rx)w'\dot{w}'(\dot{\theta}_1 \\ + \dot{\theta}_2)\Big)dx \\ = \tau_2 \quad (8)\end{aligned}$$

$$\begin{aligned}\rho A(r+x)(\ddot{\theta}_1+\ddot{\theta}_2) + \rho\ddot{w} + \rho L_1(\ddot{\theta}_1+\ddot{\theta}_2)\cos(\theta_2) \\ - \rho w(\dot{\theta}_1+\dot{\theta}_2)^2 + \rho L_1\dot{\theta}_1^2\sin(\theta_2) \\ + EI_2 w'''' - \Big(\frac{1}{2}\rho(\dot{\theta}_1+\dot{\theta}_2)^2(L_2^2 \\ - x^2) + \rho(\dot{\theta}_1+\dot{\theta}_2)^2 r(L_2-x)\Big)w'' \\ + \rho(\dot{\theta}_1+\dot{\theta}_2)^2(x+r)w' \\ = 0 \quad (9)\end{aligned}$$

The assumed modes method is used to approximate $w(x,t)$. The relative motion of the flexible link with respect to the rotating

ISSN: 1992-8645 www.jatit.org E-ISSN: 1817-3195

reference $(x, y, Z)$ system will be written in terms of the first modal coordinate $q_1(t)$ and the clamped-free beam's first mode shape $\varphi_1(x)$ :

$$w(x,t) = q_1(t)\varphi_1(x) \tag{10}$$

Where :

$$\varphi_1(x) = sin(px) - \sigma\, cos(px) \\ -sin\, h(px) \quad + cos\, h(px) \tag{11}$$

$$p = \frac{\sqrt{3.5160}}{L_2} \tag{12}$$

And

$$\sigma = \frac{sin(pL_2) + sin\, h(pL_2)}{cos(pL_2) + cos\, h(pL_2)} \tag{13}$$

Applying the above mentioned equations of motion yelds the following non-linear coupled set of ordinnary differential equations:

$$M(q)\ddot{q} + h(q,\dot{q}) + K(q) = u(t) \tag{14}$$

Where $q$ is the vector of generalised cordinates representing the rigid-body and the elastic degrees of freedom, and $u(t)$ is the vector of external forces.

$$q = [\theta_1 \quad \theta_2 \quad q_1]^T \tag{15}$$

$$u(t) = [\tau_1 \quad \tau_2 \quad 0]^T \tag{16}$$

Matrices $M(q)$ and $K(q)$ are respectively the mass and the stiffness ones, and the vector $h(q, \dot{q})$ regroups the nonlinear centrifugal and Coriolis terms.

In addition, the shoulder servomotor viscous friction coefficient $\alpha_m$ and the flexible link structural damping can form a modal damping matrix $H_d$ as [20]:

$$H_d = \begin{bmatrix} \alpha_m & 0 \\ 0 & 2\xi_1 m_{22}\omega_1 \end{bmatrix} \tag{17}$$

Where $\omega_1$ is the first elastic mode natural frequency, and $\xi_1$ its respective modal damping coefficient. Coefficient $m_{22}$ is the corresponding element of the mass matrix $M(q)$. All the matrices and vectors, with their numerical values used for simulation, are presented in the appendix.

## 3. THE EXTENDED AND UNSCENTED KALMAN FILTERS

The Extended Kalman Filter (EKF) and the Unscented Kalman Filter (UKF) evaluate the probability distribution function (pdf) of a random variable as it undergoes a nonlinear transformation.

This section deals with the EKF and UKF principles and algorithms. It summarizes the prediction/correction estimation steps given the additive process and measurements noises assumption.

### 3.1 The Extended Kalman Filter Principle and Algorithm

At each discrete time step, the EKF propagates the pdf of a random vector using a linear approximation of the nonlinear system around the operating point. The Taylor series expansion is used, and the jacobians required make the filter prohibitively difficult to implement especially when the system is of higher order.

The design of the EKF is based on the following continuous-time, nonlinear stochastic system:

$$\begin{cases} \dot{x} = f(x,u) + \eta \\ y = h(x) + v \end{cases} \tag{18}$$

where $x \in \mathbb{R}^n$ is the system state, $u \in \mathbb{R}^p$ the input, $y \in \mathbb{R}^m$ the output and $\eta \in \mathbb{R}^n$ and $v \in \mathbb{R}^m$ the process and observation noise functions respectively.

The noises are assumed to be continuous-time, white, zero-mean, uncorrelated and have covariance matrices $Q \in \mathbb{R}^{n\times n}$ and $R \in \mathbb{R}^{m\times m}$ respectively.

$$\begin{cases} E\big[(\eta(t))(\eta(\tau))\big] = Q\delta(t-\tau) \\ E\big[(v(t))(v(\tau))\big] = R\delta(t-\tau) \end{cases} \tag{19}$$

Where $E[.]$ and $\delta(.)$ are, respectively, the expected value and the continuous-time impulse function.

To identify the operating point, the state nominal trajectory is the state estimate $x_0 = \hat{x}$, while the nominal trajectories of the process and measurement noises are equal to zero as they are assumed to be zero-mean signals. The control signal is deterministic, and its nominal trajectory is assumed to be the control signal itself $u_0(t) = u(t)$.

Linearizing both the prediction and the output functions, $f(x,u)$ and $h(x)$, around the nominal trajectories yields:

$$f(x,u) = f(x_0,u,\eta_0) + \left.\frac{\partial f}{\partial x}\right|_0 (x-x_0) = f(x_0,u,w_0) + \nabla F_x(x-x_0) \quad (20)$$

$$h(x) = h(x_0) + \left.\frac{\partial h}{\partial x}\right|_0 (x-x_0) = h(x_0,v_0) + \nabla H_x(x-x_0) \quad (21)$$

The EKF equations are then given by [9]:

$$\hat{x}(0) = E[x(0)] \quad (22)$$
$$P(0) = E\left[\big(x(0)-\hat{x}(0)\big)\big(x(0)-\hat{x}(0)\big)^T\right] \quad (23)$$
$$\dot{\hat{x}} = f(\hat{x},u,\eta_0) + K\big(y - h(\hat{x},\eta_0)\big) \quad (24)$$
$$K = P\,\nabla {H_x}^T R^{-1} \quad (25)$$
$$\dot{P} = \nabla F_x P + P\nabla {F_x}^T + Q - P\nabla {H_x}^T R^{-1}\nabla H_x P \quad (26)$$

Where P is the covariance of the estimation error.

## 3.2 The Unscented Kalman Filter Principle and Algorithm

The Unscented Kalman Filter (UKF) uses a statistical linearization as an alternative to the analytical one used in the EKF algorithm. The unscented transform propagates the pdf in a simple and effective way and it is accurate up to second order in estimating mean and covariance [13]. This transformation uses $(2n+1)$ selected points, called the sigma-points that are deterministically chosen to completely capture the true mean and covariance of the states. Those points are then propagated through the nonlinear prediction and output functions. The transformed points are then used to calculate a weighted sample mean and covariance.

We consider the same nonlinear system described by (18). The standard UKF state estimation algorithm initialise the state, the initial error covariance, the process noise and the measurement noise covariance matrices as for the EKF.

At each discrete time $k$, the sigma-points are generated, using the covariance matrix square root $\left(\sqrt{P}\right)$, usually using the Cholesky method, as follows:

$$\chi_{k-1} = \begin{bmatrix} \hat{x}_{k-1} \\ \hat{x}_{k-1} + \sqrt{(N+\kappa)}\sqrt{P_{k-1}}_{(i)} \\ \hat{x}_{k-1} - \sqrt{(N+\kappa)}\sqrt{P_{k-1}}_{(i)} \end{bmatrix}^T \quad (27)$$

Where $\sqrt{P_{k-1}}_{(i)}$ is the $i^{th}$ row of the covariance matrix square root defined as $\sqrt{P}^T\sqrt{P} = P$ [21].

Once, the sigma-points are propagated through the prediction nonlinear function, the mean and covariance of the predicted state are calculated as follows [21]:

$$\dot{\chi}^{(i)}_{k/k-1} = f(\chi_{k-1},u_{k-1}) \quad i = 0\cdots 2n_x \quad (28)$$

$$\hat{x}_{k/k-1} = \sum_{i=0}^{2n} w_i\,\chi^{(i)}_{k/k-1} \quad (29)$$

$$P_{k/k-1} = Q_{k-1} + \sum_{i=0}^{2n} w_i\left(\chi^{(i)}_{k/k-1} - \hat{x}_{k/k-1}\right)\left(\chi^{(i)}_{k/k-1} - \hat{x}_{k/k-1}\right)^T \quad (30)$$

Where the weight coefficients $w_i$ are given by:

$$\begin{cases} w_0 = \dfrac{\kappa}{\kappa+n} \\ w_i = \dfrac{1}{2(\kappa+n)} \quad i = 1\cdots 2n \end{cases} \quad (31)$$

The parameter $\kappa$ is used to reduce the overall estimation error, yet its value must garantee the covariance matrix to remain positive definite. It's recommanded value is $3-n$ if the system is of lower order. Otherwise, it's set to zero.

The sigma-points are also propagated through the nonlinear outut function:

$$\psi^{(i)}_{k/k-1} = h(\chi^{(i)}_{k/k-1},u_k) \quad i = 0\cdots 2n \quad (32)$$

And the mean and covariance of predicted output are then calculated:

$$\hat{y}_{k/k-1} = \sum_{i=0}^{2n} w_i\,\psi^{(i)}_{k/k-1} \quad (33)$$

$$P_k^{yy} = R_k + \sum_{i=0}^{2n} w_i\left(\psi^{(i)}_{k/k-1} - \hat{y}_{k/k-1}\right)\left(\psi^{(i)}_{k/k-1} - \hat{y}_{k/k-1}\right)^T \quad (34)$$

The cross-covariance of state and output is calculated as:

ISSN: 1992-8645 www.jatit.org E-ISSN: 1817-3195

$$P_k^{xy} = \sum_{i=0}^{2n} w_i \left(\chi_{k/k-1}^{(i)} - \hat{x}_{k/k-1}\right) (\psi_{k/k-1}^{(i)} - \hat{y}_{k/k-1})^T \quad (35)$$

Finally, the state and covariance are updated for the next discrete time after the Kalman gain is evaluated.

$$K_k = P_k^{xy}\left(P_k^{yy}\right)^{-1} \quad (36)$$

$$\hat{x}_k = \hat{x}_{k/k-1} + K_k\left(y_k - \hat{y}_{k/k-1}\right) \quad (37)$$

$$P_k = P_{k/k-1} - K_k P_k^{yy} {K_k}^T \quad (38)$$

## 4. SIMULATION RESULTS

The state variables to estimate are the shoulder angle $\theta_1(t)$, the elbow angle $\theta_2(t)$, the first modal coordinate $q_1(t)$ and their respective time derivatives.

The system has two inputs which are the mechanical shoulder and elbow torques $\tau_1(t)$ and $\tau_2(t)$, and three accessible noisy outputs $\theta_1(t)$, $\theta_2(t)$, and $q_1(t)$.

The EKF and UKF numerical algorithms were implemented in Matlab environment, while the model simplifying and the jacobians derivation was carried out using the Mathematica packages. The nonlinearities of the process model requires a relatively small time steps for numerical integration. It's been set to $0.001$ s, and the measurement update frequency of the filters coincides with the system discretization sampling frequency.

*Table 1: Numerical Parameters of the System*

| | | |
|---|---|---|
| **Rigid link** | Mass | $m_1 = 1\ Kg$ |
| | Length | $L_1 = 0.5\ m$ |
| | Inertia | $I_1 = 0.0834\ Kg.m^2$ |
| **Flexible link** | Length | $L_2 = 0.5\ m$ |
| | Mass density per unit length | $\rho A = 0.15\ Kg.m^{-1}$ |
| | Flexural rigidity | $EI_2 = 1\ N.m^2$ |
| | Quadratic moment | $I = 1.45\ 10^{-9}\ m^4$ |
| | First mode damping coefficient | $\xi_1 = 0.01\ m$ |
| | First mode damping coefficient | $\omega_1 = 36.3131\ rad/s$ |
| **Elbow hub** | Radius | $r = 0.04\ m$ |
| | Mass | $m_h = 0.5\ Kg.m^2$ |
| **Shoulder servomotor and hub** | Inertia | $I_h = 0.002\ Kg.m^2$ |
| **Elbow servomotor** | Viscous friction coefficient | $\alpha_m = 0.95\ Nm.rd^{-1}.s^{-1}$ |

Table 1 shows the links, hubs and servomotors parameters needed for the numerical simulation, and Figure 2 to Figure 4 show respectively the control torques used for the simulation and the noisy measurement used for the state estimate update for the small noise case and for the large noise case.

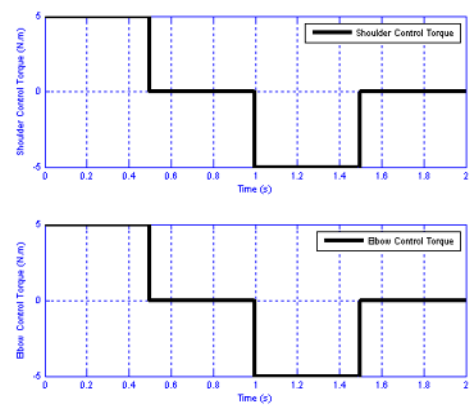


*Figure 2: Shoulder and Elbow Control Torques*

ISSN: 1992-8645 www.jatit.org E-ISSN: 1817-3195

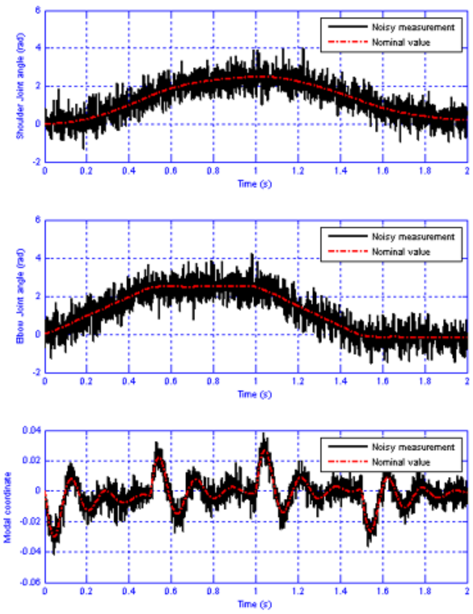

*Figure 3: Nominal and Noisy measurements for the Small Noise Case*

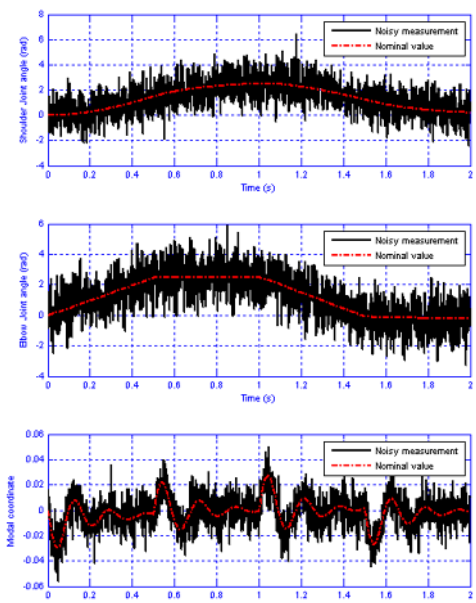

*Figure 4: Nominal and Noisy measurements for the Large Noise Case*

For the two cases, the simulations have been conducted given the following assumptions:

- Both the process noise and the measurement noise are Gaussian, zero-mean, white and with known covariance matrices.

- The EKF and the UKF models used for estimation are always the same, and they are perfectly equal to the truth model.

- The initial state and process/measurement noise covariances are the same for both the EKF and UKF.
- The truth model initial state is chosen as :
  $$x_0 = [\theta_{10} \quad \theta_{20} \quad q_{10} \quad \dot{\theta}_{10} \quad \dot{\theta}_{20} \quad \dot{q}_{10}]^T = [0]_{6\times 1}$$
  While both filters algorithms suppose the following initial state:
  $$\hat{x}_0 = \left[\hat{\theta}_0 \quad \hat{\theta}_0 \quad \hat{q}_{10} \quad \hat{\dot{\theta}}_0 \quad \hat{\dot{\theta}}_0 \quad \hat{\dot{q}}_{10}\right]^T = [4 \quad 4 \quad 0.1 \quad 2 \quad 2 \quad 0.2]^T$$
- For the UKF algorithm, the weight coefficients are:
  $$\begin{cases} w_0 = 0 \\ w_i = \dfrac{1}{2n} \quad i = 1 \cdots 2n \end{cases}$$
  The parameter κ was set to zero.
- The initial error covariance is assumed to be:
  $P(0) = \hat{x}_0\hat{x}_0{}^T$ for the EKF.
  $P(0) = 10\, I_{6\times 6}$ for the UKF.

- The process noise and measurement noise covariance matrices are respectiveley given by:
  $Q = 0.1\, I_{6\times 6}$for the samll noise case.
  $Q = I_{6\times 6}$ for the large nois case.
  $R = 0.5\, Diag_{3\times 3}(1,1,10^{-4})$ for the samll noise case.
  $R = Diag_{3\times 3}(1,1,10^{-4})$ for the large noise case.

- The update period of the simulation is $0.001\ s$, and the simulation time is 2s.

One can notice from the displayed results that both the EKF and the UKF state estimates converge to the true state.

According to Figures 5 to 10, the UKF required time to converge is lower compared to the EKF one either if corrupting noises are assumed to be small or large. The prediction function jacobians is repeatedly evaluated at each time step which is time consuming for the second algorithm.

ISSN: 1992-8645 www.jatit.org E-ISSN: 1817-3195

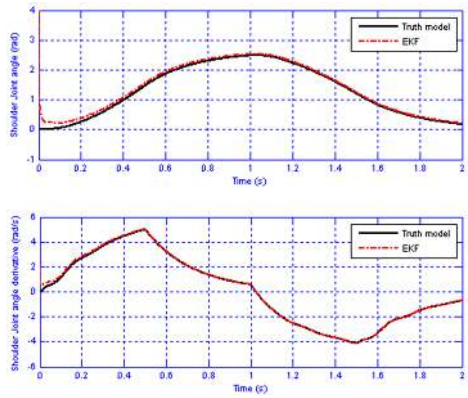


*Figure 5: Shoulder Angle Estimation for the Small Noise Case Using the EKF*

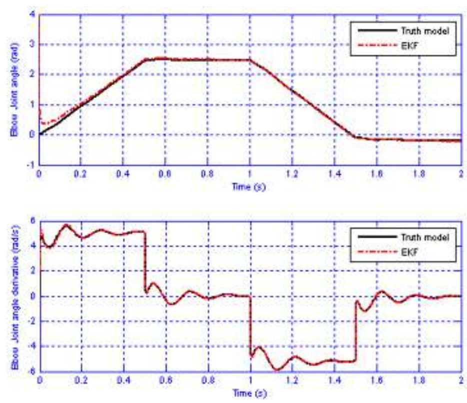


*Figure 6: Elbow Angle Estimation for the Small Noise Case Using the EKF*

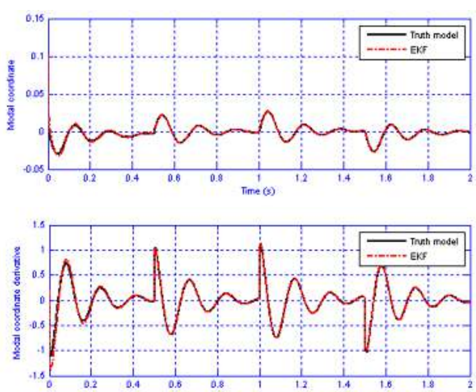


*Figure 7: Modal Coordinate Estimation for the Small Noise Case Using the EKF*

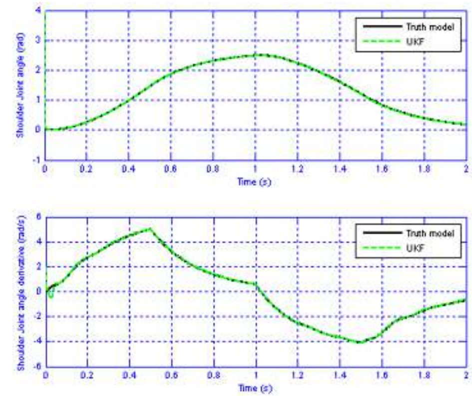


*Figure 8: Shoulder Angle Estimation for the Small Noise Case Using the UKF*

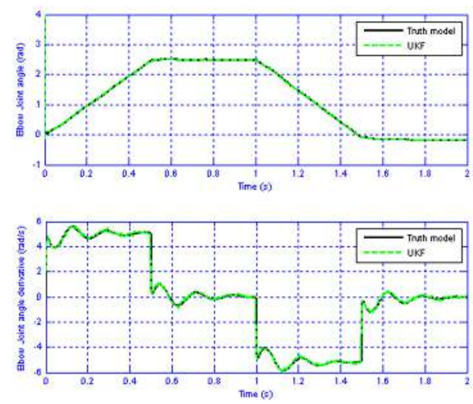


*Figure 9: Elbow Angle Estimation for the Small Noise Case Using the UKF*

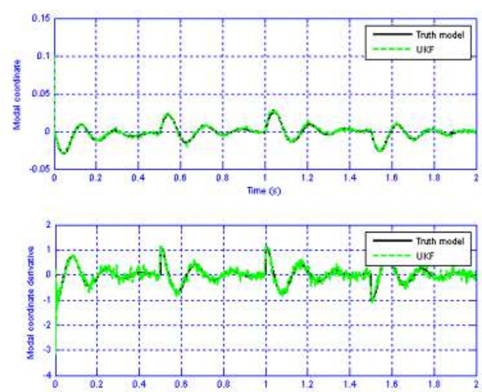


*Figure 10: Modal Coordinate Estimation for the Small Noise Case Using the UKF*

Journal of Theoretical and Applied Information Technology
15th February 2017. Vol.95. No.3

ISSN: 1992-8645 www.jatit.org E-ISSN: 1817-3195

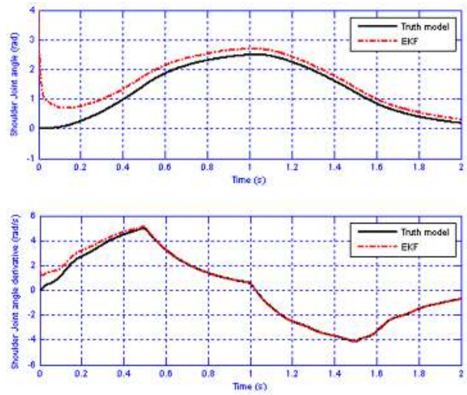

Figure 11: Shoulder Angle Estimation for the Large Noise Case Using the EKF

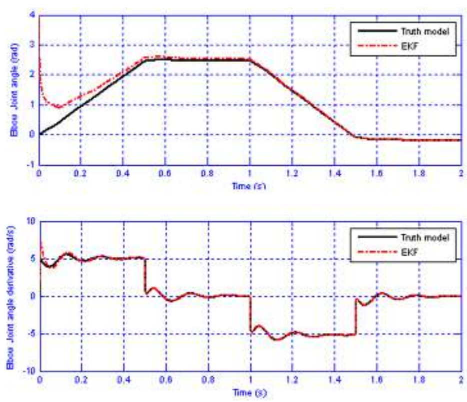

Figure 12: Elbow Angle Estimation for the Large Noise Case Using the EKF

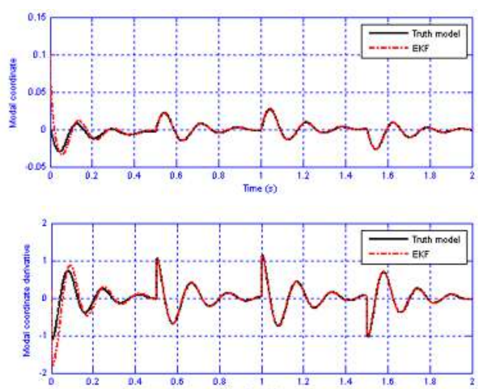

Figure 13: Modal Coordinate Estimation for the Large Noise Case Using the EKF

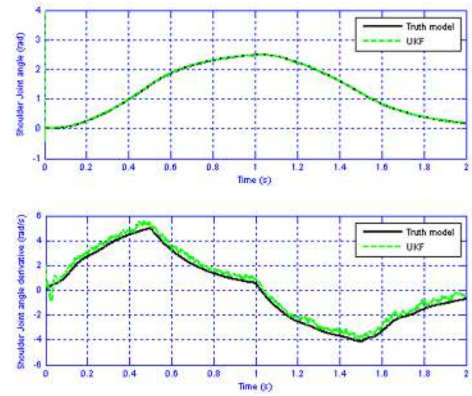

Figure 14: Shoulder Angle Estimation for the Large Noise Case Using the UKF

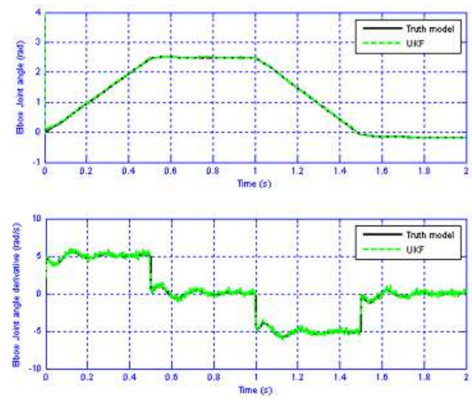

Figure 15: Elbow Angle Estimation for the Large Noise Case Using the UKF

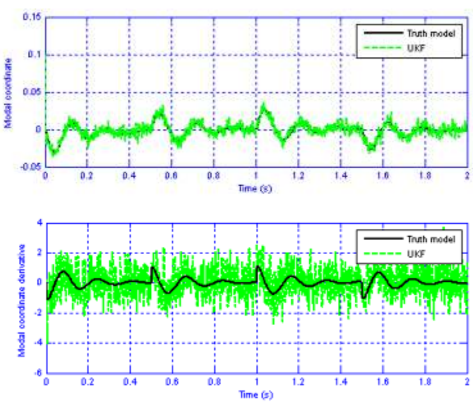

Figure 16: Modal Coordinate Estimation for the Large Noise Case Using the UKF

However, and according to Figures 11 to 16, it's clear that large noises make the UKF results less accurate, especially when estimating the time derivative state variables.

In order to quantify the filters performance, an important measure is the Root Mean Squared Error (RMSE). It is calculated for each state variable $x_i$ as follows:

ISSN: 1992-8645 www.jatit.org E-ISSN: 1817-3195

$$RMSE(x_i) = \sqrt{\frac{1}{N_s}\sum_{k=1}^{N_s}(\hat{x}_i - x_i)^2} \quad (39)$$

Where $N_s$ is the number of samples.

According to the results, displayed by Table 2 and Table 3, a clear performance advantage is demonstrated for the UKF when estimating the shoulder angle, the elbow angle and the modal coordinate, while the EKF is more accurate when estimating their respective time derivatives. This is true either when large or small noises are corrupting the system dynamics or the avilable measurements.

*Table 2: Root Mean Square Error for Small Measurements noise*

| | EKF | UKF |
|---|---|---|
| $\theta_1(t)$ | 0,02512 | **0,00821** |
| $\theta_2(t)$ | 0,01877 | **0,00839** |
| $q_1(t)$ | 9,08194 $10^{-6}$ | **6,95817 $10^{-6}$** |
| $\dot{\theta}_1(t)$ | 0,01050 | **0,01025** |
| $\dot{\theta}_2(t)$ | **0,00895** | 0,016215 |
| $\dot{q}_1(t)$ | **0,00203** | 0,01344 |

*Table 3: Root Mean Square Error for Large Measurements noise*

| | EKF | UKF |
|---|---|---|
| $\theta_1(t)$ | 0,13043 | **0,00855** |
| $\theta_2(t)$ | 0,08667 | **0,01077** |
| $q_1(t)$ | 2,95858 $10^{-5}$ | **2,77229 $10^{-5}$** |
| $\dot{\theta}_1(t)$ | **0,06264** | 0,22809 |
| $\dot{\theta}_2(t)$ | **0,04490** | 0,06881 |
| $\dot{q}_1(t)$ | **0,01290** | 0,81582 |

## 5. CONCLUSION

This paper considers the problem of nonlinear filtering for the 2 Degrees of Freedom (2DOF) Rigid-flexible manipulator state estimation. An exact dynamic model of the manipulator moving in a horizontal plane is derived using the Hamilton's principle and the assumed modes method considering the first elastic mode.

The paper main contribution is to evaluate the ability of the Extended and Unscented Kalman filters when used to give a state estimate based on the available noisy measurements. The discussion concerns both the large and small noises assumptions.

According to the simulation results, the required time for the error to converge is lowered with the UKF when the process/measurements noises are assumed to be small. The EKF is better facing large noises.

The RMSE criterion is used to quantify the estimation error. The numerical results demonstrate that the UKF outperforms the EKF when estimating the shoulder angle, the elbow angle and the modal coordinate. The EKF is sensibly more accurate when estimating their respective time derivatives.

## REFERENCES

[1] Shitole C. and Sumathi P., "Sliding DFT-based vibration mode estimator for single-link flexible manipulator", *IEEE/ASME Transactions on Mechatronics*, Vol. 20, No. 6, 2015, pp. 3249-3256.

[2] Dwivedy S.K. and Eberhard P. "Dynamic analysis of flexible manipulators, a literature review", *Mechanism and Machine*, Vol. 41, No. 7, 2006, pp. 749-777.

[3] Mosayebi M., Ghayour M. and Sadigh M.J., "A nonlinear high gain observer based input–output control of flexible link manipulator", *Mechanics Research Communications*, Vol. 45, 2012, pp. 34–41.

[4] Kurode S. and Merchant M., "Observer based control of flexible link manipulator using discrete sliding modes", *Proceedings of IEEE International Conference on Control Application (Hyderabad),* August 28-30, 2013, pp. 276–281.

[5] Yang H., Liu J. and Lan X., "Observer design for a flexible-link manipulator with PDE model", *Journal of Sound and Vibration*, Vol. 341, No. 14, 2015, pp. 237–245.

[6] Jiang T., Liu J. and He W., "Boundary control for a flexible manipulator based on infinite dimensional disturbance observer", *Journal of Sound and Vibration*, Vol. 348, No. 21, 2015, pp. 1-14.

[7] Talole S.E., Kolhe J.P. and Phadke S.B., "Extended-state-observer-based control of flexible-joint system with experimental validation", *IEEE Transactions on Industrial Electronics*, Vol. 57, No. 4, 2010, pp. 1411–1419.

ISSN: 1992-8645 www.jatit.org E-ISSN: 1817-3195

[8] Atashzar S.F., Talebi H.A., Towhidkhah F. and Shahbazi M., "Tracking control of flexible-link manipulators based on environmental force disturbance observer", *Proceedings of the 49th IEEE Conference on Decision and Control, (Atlanta, GA),* December 15-17, 2010, pp. 3584–3589.

[9] Simon D., "Optimal State Estimation: Kalman, H Infinity, and Nonlinear Approaches", John Wiley & Sons, Inc, 2006.

[10] Kushner H.J., "Dynamical equations for optimal nonlinear filtering", *Journal of Differential Equations*, Vol. 3, No. 2, 1967, pp. 179–190.

[11] Walpole R.E., Myers R.H., Myers S.L., and Ye K., "Probability & Statistics for Engineers & Scientists", Prentice Hall, Boston, 2012.

[12] Chui C.K. and Chen G., "Kalman filtering with real-time applications", Springer, Berlin, 2009.

[13] Julier S.J. and Uhlmann J.K., "Unscented filtering and nonlinear estimation", *Proceedings of IEEE,* Vol. 92, No. 3, 2004, pp. 401-422.

[14] M. BAKHTI & B. B. IDRISSI, "Highly Nonlinear Flexible Manipulator State Estimation Using the Extended and the Unscented Kalman Filters", *International Review of Automatic Control (IREACO)*, Vol.9, No.03, 2016, pp. 151-160.

[15] M. BAKHTI & B. B. IDRISSI, "Nonlinear One Link Flexible Manipulator State Estimation Using the Extended Kalman Filter", *International Journal of Control and Automation*, Vol. 9, No. 11, 2016, pp. 315-326.

[16] M. BAKHTI & B. B. IDRISSI, "Active Vibration Control of a Flexible Manipulator Using Model Predictive Control and Kalman Optimal Filtering", *International Journal of Engineering Science and Technology,* Vol. 5, No. 1, 2013, pp. 165-177.

[17] Tokhi M.O. and Azad A.K.M. "Flexible Robot Manipulators Modelling, simulation and control", The Institution of Engineering and Technology, 2008.

[18] Yigit A.S., Scott R.A., and Ulsoy A.G., "Flexural motion of a radially rotating beam attached to a rigid body", *Journal of Sound and Vibration*, Vol. 121, No. 2, 1988, pp. 201-210.

[19] Dym C. L. and Shames I. H., "Solid mechanics, a variational approach", Springer, New York, 2013.

[20] Hassan M., Dubay R., Li C. and Wang R., "Active vibration control of a flexible one-link manipulator using a multivariable predictive controller", *Mechatronics*, Vol. 17, No. 6, 2007, pp. 311–323.

[21] Julier S.J., Uhlmann J.K. and Durrant-Whyte H.F, "A new method for the nonlinear transformation of means and covariances in filters and estimators", *IEEE Transactions on Automatic Control*, Vol. 45, No. 3, 2000, pp. 477-482.

Journal of Theoretical and Applied Information Technology
15th February 2017. Vol.95. No.3

ISSN: 1992-8645 www.jatit.org E-ISSN: 1817-3195

**APPENDIX**

### MODEL MATRICES AND VECTORS EXPRESSIONS WITH NUMERICAL VALUES

The elements of the symmetric mass matrix:

$$M(q) = [m_{ij}]_{3\times3}$$

$$m_{11} = I_h + \int_0^{L_2} \rho A (x+r)^2 dx + \rho A L_1^2 L_2 + 2\left(\frac{1}{2}\rho A L_1^2 L_2 + \rho A L_1 L_2 r\right) cos(\theta_2) + I_1 + m_h L_1^2 - 2L_1 sin(\theta_2)\left(\int_0^{L_2} \rho A \varphi_1(x) dx\right) q_1$$

$$m_{11} = 0.2370 + 0.0218\cos(\theta_2) - 0.08 q_1 \sin(\theta_2)$$

$$m_{12} = I_h + \int_0^{L_2} \rho A (x+r)^2 dx + \left(\frac{1}{2}\rho A L_1^2 L_2 + \rho A L_1 L_2 r\right) cos(\theta_2) - L_1 sin(\theta_2)\left(\int_0^{L_2} \rho A \varphi_1(x) dx\right) q_1$$

$$m_{12} = 0.0099 + 0.0109\cos(\theta_2) - 0.04 q_1 \sin(\theta_2)$$

$$m_{13} = \int_0^{L_2} \rho A (x+r)\varphi_1(x) dx + L_1\left(\int_0^{L_2} \rho A \varphi_1(x) dx\right) cos(\theta_2)$$

$$m_{13} = 0.0323 + 0.04\cos(\theta_2)$$

$$m_{22} = I_h + \int_0^{L_2} \rho A (x+r)^2 dx$$

$$m_{22} = 0.0099$$

$$m_{23} = \int_0^{L_2} \rho A (x+r)\varphi_1(x) dx$$

$$m_{23} = 0.0323$$

$$m_{33} = \int_0^{L_2} \rho A \left(\varphi_1(x)\right)^2 dx$$

$$m_{33} = 0.1392$$

The elements of the diagonal stiffness matrix:

$$K(q) = [k_{ij}]_{3\times3}$$

$$k_{11} = k_{12} = 0$$

$$k_{33} = \int_0^{L_2} EI_2 \left(\frac{\partial^2 v}{\partial x^2}\right)^2 dx$$

$$k_{33} = 183.52$$

The elements of vector:

$$h(q, \dot{q}) = [h_i]_{3\times1}$$

$$h_1 = -\left(\left(\frac{1}{2}\rho A L_1^2 L_2 + \rho A L_1 L_2 r\right)\sin(\theta_2) + L_1 cos(\theta_2)\left(\int_0^{L_2} \rho A \varphi_1(x) dx\right) q_1\right)\dot{\theta}_2^2 - \left(2\left(\frac{1}{2}\rho A L_1^2 L_2 + \rho A L_1 L_2 r\right) sin(\theta_2) + 2L_1 cos(\theta_2)\left(\int_0^{L_2} \rho A \varphi_1(x) dx\right) q_1\right)\dot{\theta}_1\dot{\theta}_2 - 2L_1 sin(\theta_2)\left(\left(\int_0^{L_2} \rho A \varphi_1(x) dx\right)\dot{q}_1\right)(\dot{\theta}_1 + \dot{\theta}_2)$$

$$h_1 = \dot{\theta}_2^2(-0.04 q_1 \cos(\theta_2) - 0.0109\sin(\theta_2)) - \dot{\theta}_1\dot{\theta}_2(q_1\cos(\theta_2) + 0.0218\sin(\theta_2)) - 0.08(\dot{\theta}_1 + \dot{\theta}_2)\sin(\theta_2)$$

$$h_2 = \left(\left(\frac{1}{2}\rho A L_1^2 L_2 + \rho A L_1 L_2 r\right)\sin(\theta_2) + L_1 cos(\theta_2)\left(\int_0^{L_2} \rho A \varphi_1(x) dx\right) q_1\right)\dot{\theta}_1^2$$

$$h_2 = \dot{\theta}_1^2(0.04\, q_1\, cos(\theta_2) + 0.0109\, sin(\theta_2))$$

$$h_3 = \left(\int_0^{L_2}\left(\rho A (x+r)\varphi_1'^{(x)}\varphi_1(x) - \frac{1}{2}\rho A (L_2^2 - x^2 + 2rL_2 - 2rx)\varphi_1''(x)\varphi_1(x)\right) dx - I_h - \int_0^{L_2} \rho A (x+r)^2 dx - \rho A L_1^2 L_2 - 2\left(\frac{1}{2}\rho A L_1^2 L_2 + \rho A L_1 L_2 r\right) cos(\theta_2) - I_1 - m_h L_1^2 + 2L_1 sin(\theta_2)\left(\int_0^{L_2} \rho A \varphi_1(x) dx\right) q_1\right) q_1(\dot{\theta}_1 + \dot{\theta}_2)^2 + \left(\int_0^{L_2} \rho A \varphi_1(x) dx\right) q_1 L_1 \sin(\theta_2)\, \theta_1^2$$

$$h_3 = 0.0444\, q_1(\dot{\theta}_1 + \dot{\theta}_2)^2 + 0.04\dot{\theta}_1^2 \sin(\theta_2)$$

The elements of the diagonal damping matrix:

$$H_d(q) = [hd_{ij}]_{3\times3}$$

$$hd_{11} = hd_{22} = 0.95$$

$$hd_{33} = 0.1010$$